Cancer Cell
Article

Fez1/Lzts1 Absence Impairs Cdk1/Cdc25C Interaction during Mitosis and Predisposes Mice to Cancer Development

Andrea Vecchione,[1,2,9] Gustavo Baldassarre,[3,9] Hideshi Ishii,[4] Milena S. Nicoloso,[1,3] Barbara Belletti,[3] Fabio Petrocca,[1] Nicola Zanesi,[1] Louise Y.Y. Fong,[1] Sabrina Battista,[6] Daniela Guarnieri,[5] Raffaele Baffa,[7] Hansjuerg Alder,[1] John L. Farber,[7] Peter J. Donovan,[8] and Carlo M. Croce[1,*]

[1] Department of Molecular Virology, Immunology, and Medical Genetics and Comprehensive Cancer Center, Ohio State University, Columbus, OH 43210, USA
[2] Division of Pathology, II Faculty of Medicine, University "La Sapienza," Ospedale Santo Andrea, 00185 Rome, Italy
[3] Division of Experimental Oncology, 2 CRO-IRCCS, 33081 Aviano, Italy
[4] Center for Molecular Medicine, Jichi Medical School, 329-0498 Tochigi, Japan
[5] Department of Materials and Production Engineering, University Federico II, 80139 Naples, Italy
[6] Composite and Biomedical Materials Institute, CNR, 80125 Naples, Italy
[7] Kimmel Cancer Center and Department of Pathology, Thomas Jefferson University, Philadelphia, PA 19107, USA
[8] School of Medicine, Johns Hopkins University, Baltimore, MD 21205, USA
[9] These authors contributed equally to this work.
*Correspondence: carlo.croce@osumc.edu
DOI 10.1016/j.ccr.2007.01.014

SUMMARY

The *FEZ1/LZTS1* (*LZTS1*) protein is frequently downregulated in human cancers of different histotypes. *LZTS1* is expressed in normal tissues, and its introduction in cancer cells inhibits cell growth and suppresses tumorigenicity, owing to an accumulation of cells in G2/M. Here, we define its role in cell cycle regulation and tumor progression by generating *Lzts1* knockout mice. In *Lzts1*$^{-/-}$ mouse embryo fibroblasts (MEFs), Cdc25C degradation was increased during M phase, resulting in decreased Cdk1 activity. As a consequence, *Lzts1*$^{-/-}$ MEFs showed accelerated mitotic progression, resistance to taxol- and nocodazole-induced M phase arrest, and improper chromosome segregation. Accordingly, Lzts1 deficiency was associated with an increased incidence of both spontaneous and carcinogen-induced cancers in mice.

INTRODUCTION

During the course of cancer development, a normal cell progresses toward malignancy by acquiring a specific series of mutations. Over the past decades, genetic studies have demonstrated that cancer cells accumulate DNA changes that activate oncogenes and inactivate tumor-suppressor genes.

The role of tumor-suppressor genes in neoplasia development is crucial, given that reintroduction of one or more of these genes into cells in which their function is compromised can cause complete reversion to the neoplastic process (Ichikawa et al., 1994). In light of this, it is not surprising that many tumors frequently show loss of heterozygosity (LOH) at specific chromosomal regions encompassing tumor-suppressor genes.

One of these regions is located at chromosome 8p22, which is frequently deleted in breast, lung, gastric, esophageal, prostate, and bladder cancers (Vocke et al., 1996; Wagner et al., 1997; Anbazhagan et al., 1998; El-Naggar

SIGNIFICANCE

Both entry and exit from mitosis are driven by the modulation of Cdk1 activity, which is finely regulated by several protein complexes. Knowing the players that control the activity of Cdk1 in each phase of the cell cycle is of primary importance to fully understand how normal and cancer cells divide. The present data establish *Lzts1* as an important player in ensuring proper Cdk1 activity during M phase. Lzts1 absence in a defined temporal window during M phase results in impaired Cdk1/Cdc25C interaction with a consequent drop in Cdk1 activity. During prophase and metaphase, Lzts1 protein is therefore necessary for maintaining high levels of Cdk1, which, in turn, are required for proper chromosome alignment and segregation.

et al., 1998). On the basis of this correlation and through a positional cloning strategy, we identified a novel putative tumor-suppressor gene (Ishii et al., 1999), *FEZ1/LZTS1* (*LZTS1*), which maps in this region and whose expression is altered in different human malignancies (Ishii et al., 1999; Cabeza-Arvelaiz et al., 2001; Vecchione et al., 2001, 2002; Toyooka et al., 2002; Ono et al., 2003; Nonaka et al., 2005). The reintroduction of *LZTS1* into *Lzts1* null cancer cells suppresses cell growth, and this suppression is probably mediated by *LZTS1*'s interaction with the main mitotic kinase, $p34^{cdc2}$ (hereafter referred to as Cdk1) (Ishii et al., 2001; Vecchione et al., 2002); the majority of cells are seen at the G2/M phases of the cell cycle (Ishii et al., 2001; Vecchione et al., 2002).

Cdk1 activity is finely controlled during the G2/M phases of the cell cycle, and its activity is thought to control both M phase entry and exit (reviewed in Nigg, 2001). There are multiple levels of Cdk1 activity regulation, such as binding with its regulatory subunits (Cyclins A and B), interaction with CKIs, and phosphorylation and dephosphorylation of specific residues (reviewed in Smits and Medema, 2001). Of the several proteins participating in the multifaceted Cdk1 regulation, some have been implicated in tumor progression (Carnero, 2002), directly linking proper M phase progression with cell transformation. However, the involvement of mitotic regulators in cancer is more difficult to prove since profound alterations of M phase are often not compatible with eukaryotic life (Weaver and Cleveland, 2005), a concept in line with the notion that, up to now, any effort to generate Cdk1 knockout (KO) mice has been unsuccessful. Conversely, mild alteration of M phase checkpoints often leads to aneuploidy and cell transformation (Weaver and Cleveland, 2005).

In the present study, we describe the role of the tumor-suppressor gene *Lzts1* in M phase regulation and tumor progression by utilizing *Lzts1* null mice as a model.

RESULTS

Targeted Disruption of the *Lzts1* Gene Creates a Null Allele and Favors Spontaneous Tumor Development

The mouse *Lzts1* gene was disrupted by the insertion a neomycin-resistance cassette that replaced the first *Lzts1* exon (Figure 1A). Chimeric males transmitted the mutated *Lzts1* allele through the germline, as demonstrated by Southern blot analysis of tail DNA (Figure 1B) and by reverse transcriptase-polymerase chain reaction (RT-PCR) of $Lzts1^{+/+}$, $Lzts1^{+/-}$, and $Lzts1^{-/-}$ mouse embryo fibroblasts (MEFs) (Figure 1C). $Lzts1^{-/-}$ mice arose at the expected frequency (data not shown). Western blot analysis of brain lysates from $Lzts1^{+/+}$, $Lzts1^{+/-}$, and $Lzts1^{-/-}$ mice confirmed the reduction or the absence of Lzts1 protein (Figure 1D).

Lzts1 heterozygous intercrosses were bred and observed up to 24 months of age. In animals at the age of 8–24 months (average of 16 months), pathological analysis demonstrated that 0 out of 11 $Lzts1^{+/+}$ mice, 12 out of 20 $Lzts1^{+/-}$ mice, and 9 out of 9 $Lzts1^{-/-}$ mice developed multiple tumors. The neoplasms in $Lzts1^{-/-}$ and $Lzts1^{+/-}$ mice were breast tumors, hepatocellular carcinomas, lymphomas, soft tissue sarcomas, and lung adenomas (Figures 1E–1I), a spectrum suggesting that *Lzts1* absence affects multiple cell types in vivo. Lymphomas, hepatocellular carcinomas, and soft tissue sarcomas developed at a higher penetrance in $Lzts1^{-/-}$ than in $Lzts1^{+/-}$ mice (100%, 75%, and 100% versus 35%, 50%, and 0%, respectively). Penetrance in the other histotype was not significantly different. The age of onset of the tumor was very similar in heterozygous and homozygous mice (19 ± 4.2 months for $Lzts1^{+/-}$ versus 17 ± 4.2 months for $Lzts1^{-/-}$), suggesting that one *Lzts1* allele is not sufficient and does not delay cancer development. To better address this point, we explored whether the second allele was lost in heterozygous mice. PCR experiments coupled with direct sequencing showed that the wild-type (WT) allele was neither lost nor mutated (data not shown).

$Lzts1^{-/-}$ MEFs Progress Normally through the G1, S, and G2 Phases, but Display an Altered M Phase

Our previous studies indicated that *LZTS1* is implicated in the control of cell cycle progression, since its overexpression was able to mainly block the cells in the G2/M phases, and that it probably acts on Cdk1 activity (Ishii et al., 2001; Vecchione et al., 2002). We used MEFs derived from WT or KO embryos to verify whether the mechanisms whereby Lzts1 absence predisposed mice to develop multiple tumors could be linked to its role in the control of cell cycle progression.

In growth-curve experiments, $Lzts1^{-/-}$ MEFs cultured in complete medium grew more slowly over a 6 day period when compared to $Lzts1^{+/+}$ cells (Figure 2A), probably for an increased apoptosis, as demonstrated by flow cytometry analysis (FACS) (Figure 2B) and TUNEL assay (data not shown). In order to assess if the reduced cell growth observed in $Lzts1^{-/-}$ MEFs was also due to an altered progression through the different phases of the cell cycle, we used cell synchronization to study the transition from the G1 to S phases and from the S to G2/M phases. Serum starvation followed by serum stimulation for up to 24 hr indicated that $Lzts1^{+/+}$ and $Lzts1^{-/-}$ MEFs progressed similarly from the G1 to S phases and from the S to G2 phases of the cell cycle (Figure 2C) and demonstrated similar temporal expression and phosphorylation patterns of cell cycle regulatory proteins (Figure 2D). The expression of the licensing factor Geminin, known to be expressed from the S to M phases and degraded at the metaphase-anaphase transition (McGarry and Kirschner, 1998), peaked in both cell lines 23 hr after serum stimulation; however, in cells lacking Lzts1, expression decreased rapidly (Figure 2E).

Using the double-thymidine block coupled with FACS and western blot analyses, we noted a decreased accumulation in the G2/M phases in $Lzts1^{-/-}$ compared to $Lzts1^{+/+}$ cells (Figure 3A). The observed differences in the cell cycle distribution were accompanied by slightly different expression levels of Cyclin B1 (Figure 3B), which, in $Lzts1^{+/+}$ cells, peaked from 4 to 8 hr and decreased promptly 10 hr after release and, in $Lzts1^{-/-}$ cells, rose

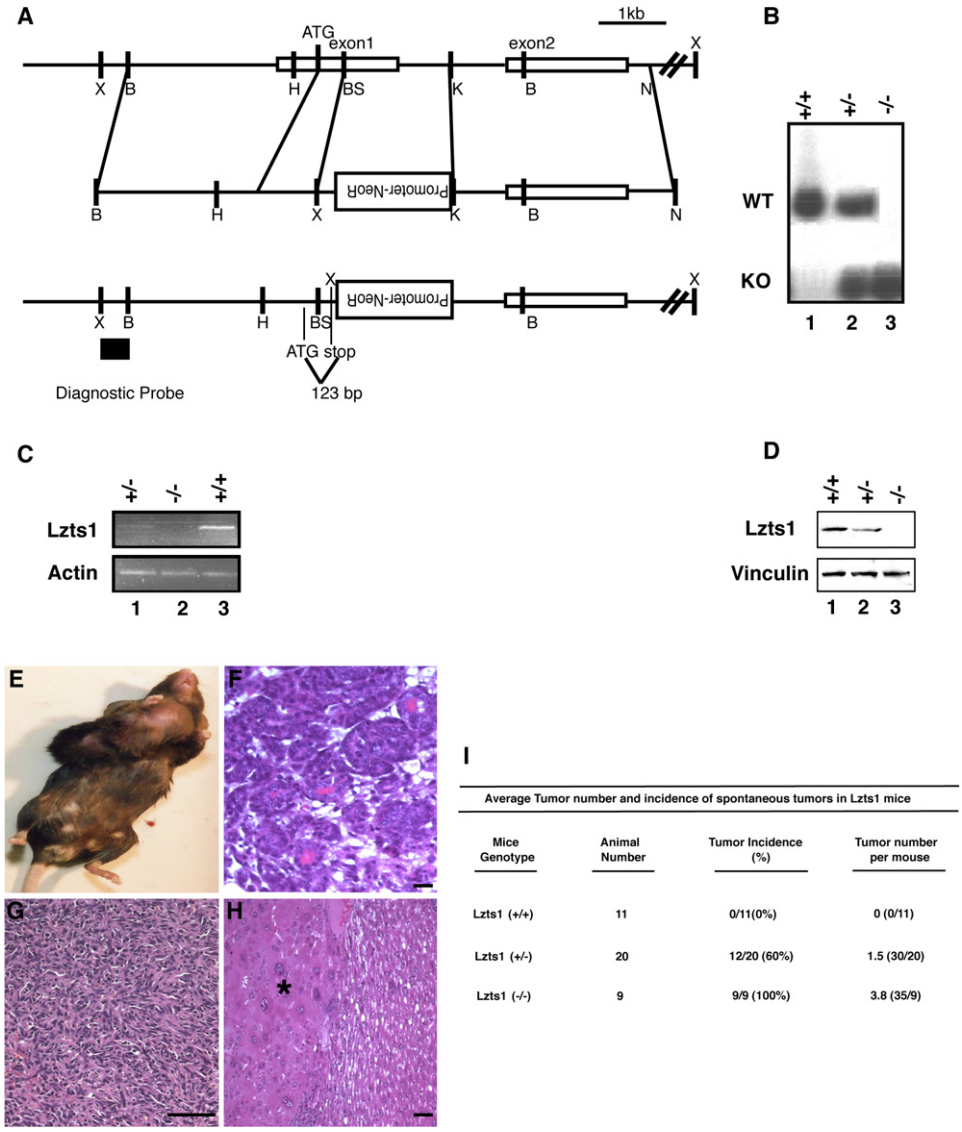

Average Tumor number and incidence of spontaneous tumors in Lzts1 mice

Mice Genotype	Animal Number	Tumor Incidence (%)	Tumor number per mouse
Lzts1 (+/+)	11	0/11(0%)	0 (0/11)
Lzts1 (+/-)	20	12/20 (60%)	1.5 (30/20)
Lzts1 (-/-)	9	9/9 (100%)	3.8 (35/9)

Figure 1. Lzts1 Knockout Mice Develop Spontaneous Tumors

(A) Targeting of the mouse *Lzts1* locus, showing that the genomic region including exons 1 and 2 of the mouse *Lzts1* gene (top) were homologously recombinant with targeting vector (middle), which results in the replacement of part of exon 1 with the neomycin-resistance gene (bottom). *Lzts1* coding was stopped 123 bp downstream of the first methionine. B, BamHI; K, KpnI; BS, Bsp106; N, NotI; H, HindIII; X, XbaI. The 600 bp diagnostic probe is located outside of the targeting vector sequence.

(B) Southern blot analysis of mouse genomic DNA, digested with XbaI and probed with the diagnostic probe depicted in (A).

(C) RT-PCR analysis showing *Lzts1* gene expression in *Lzts1*$^{+/+}$, *Lzts1*$^{+/-}$, and *Lzts1*$^{-/-}$ MEFs as indicated. Actin mRNA expression was used as a loading control.

(D) Western Blot analysis of *Lzts1* expression in brain lysates from *Lzts1*$^{+/+}$, *Lzts1*$^{+/-}$, and *Lzts1*$^{-/-}$ 15-week-old mice. Vinculin expression was used to normalize the amount of loaded proteins in each lane.

(E) Macroscopic appearance of a primary breast tumor in a *Lzts1*$^{-/-}$ mouse.

(F) Hematoxylin and eosin staining showing ductal differentiation of the breast tumor depicted in (E). The scale bar is 20 μm.

(G) High-grade sarcoma of the tight. The scale bar is 100 μm.

(H) A liver carcinoma is shown (indicated by an asterisk). The scale bar is 20 μm.

(I) Number and incidence of spontaneous tumors in the different genotypes.

at 4 hr and remained stable until 10 hr after release (Figure 3B). These data suggest two possibilities: (1) *Lzts1*$^{-/-}$ cells had a slower S to G2 progression; (2) they had a faster exit from mitosis.

To address this point, exponentially growing *Lzts1*$^{+/+}$ and *Lzts1*$^{-/-}$ cells were cultured for 1 hr in the presence of 5′-bromodeoxyuridine (BrdU), which was used to label cells in S phase. After BrdU washout, nocodazole, a drug

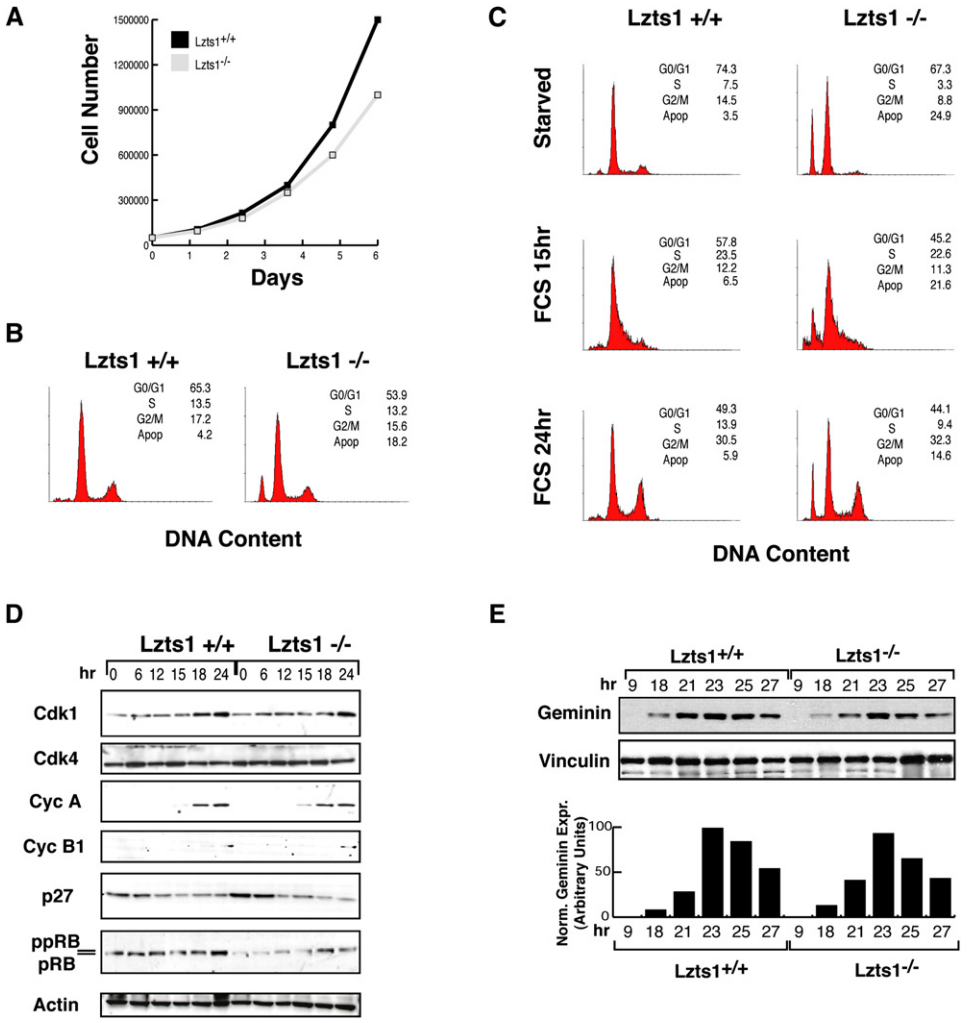

Figure 2. G1/S and S/G2 Transitions Are Not Affected by Lzts1 Absence in MEFs

(A) Growth curve comparing *Lzts1*$^{+/+}$ (black square) and *Lzts1*$^{-/-}$ (gray square) cells over the course of 6 days.

(B) FACS analysis of DNA content of *Lzts1*$^{+/+}$ and *Lzts1*$^{-/-}$ MEFs in the logarithmic phase of growth.

(C) Cell cycle distribution of *Lzts1*$^{+/+}$ and *Lzts1*$^{-/-}$ MEFs serum starved for 24 hr (starved) and then restimulated with 10% FBS-containing medium (FCS) for the indicated time.

(D) Western blot analysis of cell cycle-related proteins in *Lzts1*$^{+/+}$ and *Lzts1*$^{-/-}$ cells treated as in (C).

(E) Western blot analysis of Geminin expression in *Lzts1*$^{+/+}$ and *Lzts1*$^{-/-}$ MEFs serum starved for 24 hr (starved) and then restimulated with 10% FBS-containing medium for the indicated time. In the lower graph, the expression of Geminin normalized on the levels of vinculin at each time point is reported.

known to block cells in prometaphase, was added, and cells were collected 3, 12, and 18 hr later. FACS analysis of BrdU-positive cells showed that *Lzts1*$^{-/-}$ MEFs progressed normally from the S to G2/M phases of the cell cycle, but accumulated less efficiently in prometaphase (Figure 3C). In fact, after 12–18 hr of nocodazole treatment, 10% of *Lzts1*$^{+/+}$ versus more than 25% of *Lzts1*$^{-/-}$ MEFs were in the G1/S phases, suggesting that *Lzts1*$^{-/-}$ cells had a faster exit from mitosis after nocodazole treatment (Figure 3C).

Similar results were obtained by using a double-thymidine block followed by exposure to Hoechst 33342, which causes a reversible G2 arrest (Tobey et al., 1990). Hoechst treatment increased to ~40% in the G2 population of both *Lzts1* WT and KO MEFs (Figure 3D). After Hoechst washout, the progression through M phase was completely different since, within 2 hr, the tetraploid population remained stable in WT cells (41%) and dropped to almost half that (26.8%) in KO fibroblasts (Figure 3D). Similarly, the G1 population of WT MEFs was similar in Hoechst-blocked cells and in cells released for 2 hr (36% versus 40%, respectively), whereas the G1 population almost doubled in KO cells during the same time frame (39% versus 59% at 0 and 2 hr, respectively) (Figure 3D). During longer periods of time, both cell lines returned in G1, consistent with the reversible G2 block

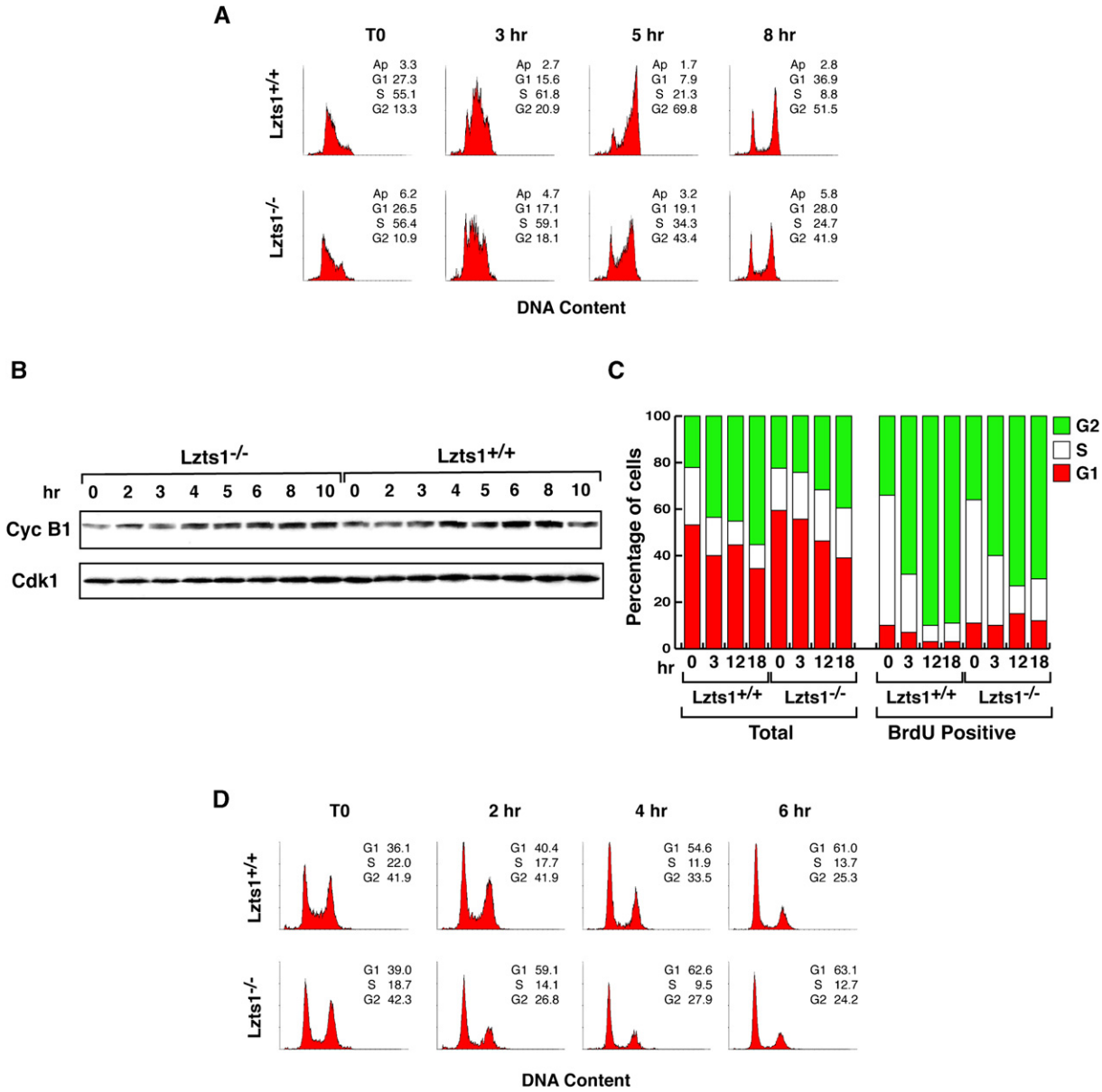

Figure 3. *Lzts1*$^{-/-}$ MEFs Displayed Mitotic Defects

(A) Flow cytometry analysis of *Lzts1*$^{+/+}$ and *Lzts1*$^{-/-}$ MEFs synchronized at the G1/S transition by a double-thymidine block and released for the indicated time.

(B) Expression of Cyclin B1 and Cdk1 proteins in cells treated as described in (A).

(C) Evaluation of cell cycle progression in cells labeled with BrdU for 1 hr and then exposed to nocodazole for the indicated time. The percentage of total or BrdU-labeled cells in each phase of the cell cycle is shown.

(D) Flow cytometry analysis of *Lzts1*$^{+/+}$ and *Lzts1*$^{-/-}$ MEFs treated for 10 hr with Hoechst 33342 (left panels, T0) and then released for the indicated time.

induced by Hoechst (Figure 3D). Altogether, these results indicate that *Lzts1* KO MEFs progressed more quickly through M phase compared to their WT counterparts.

Lzts1$^{-/-}$ MEFs Show a Faster M Phase Progression

To better study the role of Lzts1 in M phase progression, *Lzts1* WT and KO mitotic cells were isolated and analyzed for the expression of the MPM2 phosphoprotein (Westendorf et al., 1994; Shuji et al., 2001) and cell cycle distribution. Similar percentages of mitotic cells were isolated in the two cell lines (Figure 4A). The analysis of DNA content (Figure 4B) and of MPM2 expression (Figure 4C) indicated that WT MEFs arrested in prometaphase by nocodazole completed M phase within 90 min, whereas KO cells accumulated in G1 within 60 min, consistent with faster mitotic exit. Immunofluorescence analysis

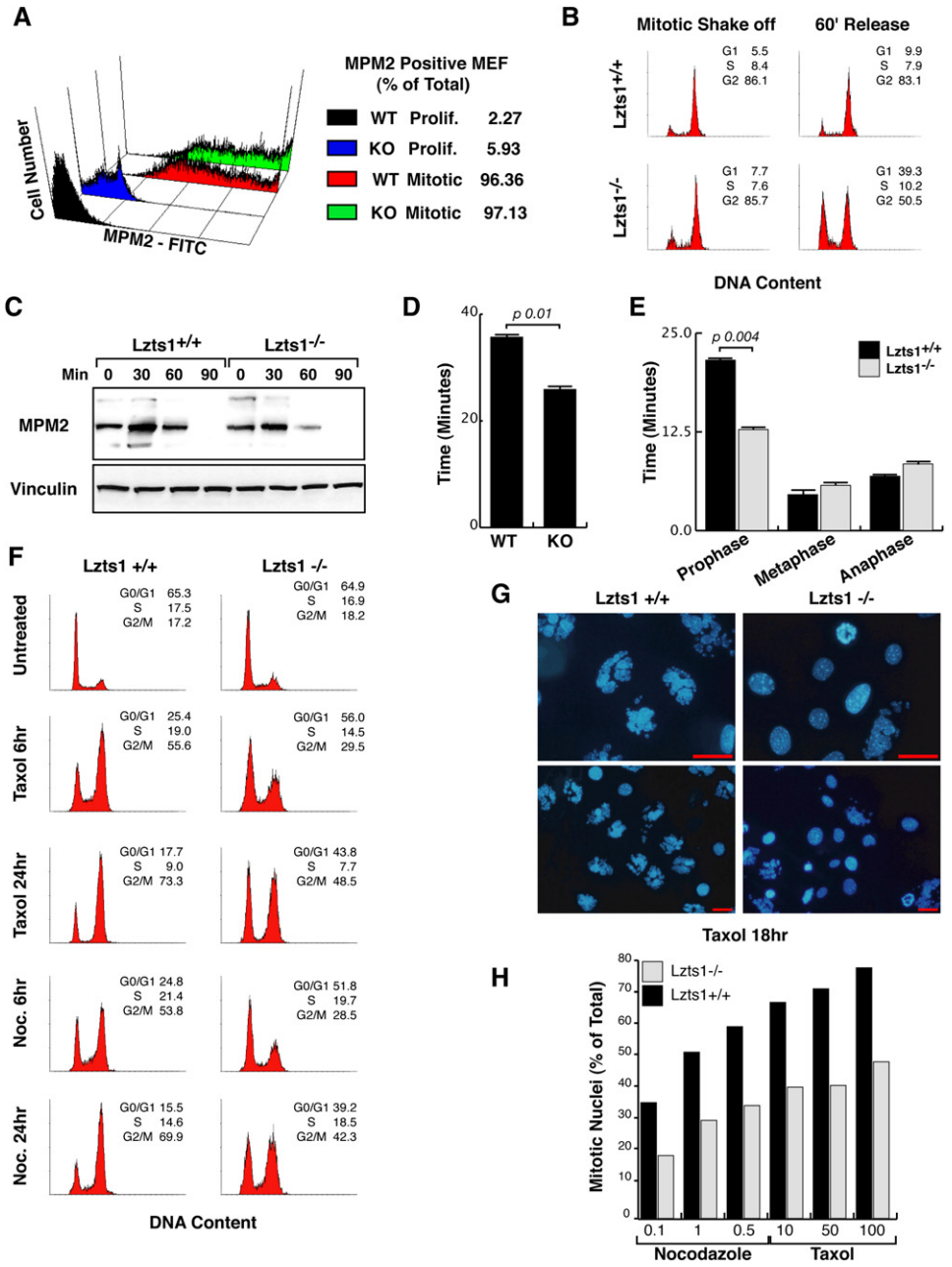

Figure 4. *Lzts1*$^{-/-}$ MEFs Displayed a Faster M Phase Progression

(A) Expression of the mitotic phosphoprotein MPM2 in proliferant and mitotic shake-off *Lzts1*$^{+/+}$ and *Lzts1*$^{-/-}$ MEFs.

(B) Flow cytometry analysis of *Lzts1*$^{+/+}$ and *Lzts1*$^{-/-}$ MEFs isolated by mitotic shake-off (left panels) and released for 60 min (right panels).

(C) Expression of the mitotic phosphoprotein MPM2 in cells collected by mitotic shake-off (0) and released for the indicated times.

(D and E) Quantification of (D) total mitosis length and of (E) time spent in each mitotic phase in *Lzts1*$^{+/+}$ and *Lzts1*$^{-/-}$ MEFs, evaluated by video time-lapse microscopy. Results (mean ± SD) are representative of eight mitotic cells (n = 8) followed independently.

(F) Flow cytometry analysis of *Lzts1*$^{+/+}$ and *Lzts1*$^{-/-}$ MEFs treated with 100 nM taxol or 1 μM nocodazole, as indicated.

(G) Hoechst nuclear staining of *Lzts1*$^{+/+}$ (left panels) and *Lzts1*$^{-/-}$ (right panels) MEFs treated for 18 hr with 100 nM taxol. Representative fields are shown. Scale bars are 20 μm.

(H) Quantification of mitotic nuclei by using Hoechst nuclear staining in cells treated as indicated. Data represent the mean of three independent experiments on two different MEF populations.

performed 90 min after the release from the nocodazole block demonstrated that the majority of WT MEFs still had the mid-body, suggesting that they were between telophase and cytokinesis; however, at the same time point, almost all KO MEFs had already divided (Figure S1A).

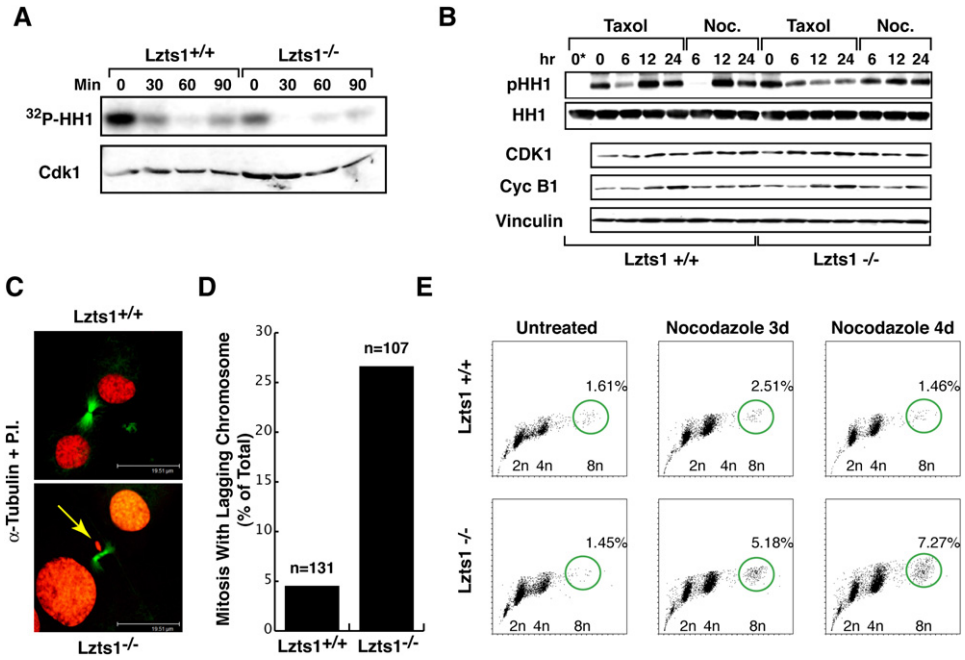

Figure 5. Lzts1 Absence Results in Decreased Cdk1 Activity and Chromosome Missegregation

(A) Cdk1-associated kinase activity in MEFs collected by mitotic shake-off (0) and released for the indicated times. The levels of Cdk1 are shown in the lower panels.

(B) Expression of Cyclin B1 and Cdk1 proteins and Cdk1-associated kinase activity in cells treated as indicated. Histone H1 (HH1) and vinculin were used to normalize the kinase assay and the proteins loaded on the blot, respectively. The 0* lane is the negative control of the kinase reaction in which the immunoprecipitated proteins have not been added.

(C) Immunofluorescence analysis of *Lzts1*$^{+/+}$ and *Lzts1*$^{-/-}$ mitotic cells stained for α-tubulin (green) and P.I. (red). A representative confocal section of a normal telophase in *Lzts1*$^{+/+}$ cells (upper panel) and of a telophase with missegregated (lagging) chromosomes (yellow arrows in the lower panel) in *Lzts1*$^{-/-}$ cells are shown. The scale bar is 19.5 μm.

(D) Quantification of mitosis presenting missegregated chromosomes in *Lzts1*$^{+/+}$ and *Lzts1*$^{-/-}$ MEFs examined 8 hr after the double-thymidine block. n is the total number of mitoses analyzed.

(E) Flow cytometry analysis of *Lzts1*$^{+/+}$ and *Lzts1*$^{-/-}$ MEFs treated with 1 μM nocodazole, as indicated. The percentage of the 8n population, representing the mean of two independent experiments on two different MEF populations, is reported.

Most of the reported experiments were conducted by utilizing nocodazole to synchronize cells in prometaphase. Since nocodazole treatment by itself has an effect on M phase length (Cimini et al., 2003), we decided to observe M phase progression in undisturbed cells by using video time-lapse microscopy. Cells were both double-thymidine blocked or left untreated, and they were followed for up to 12 hr by video microscopy, as described in Experimental Procedures. The analysis of eight WT and eight KO MEFs confirmed that in the absence of drug treatment *Lzts1*$^{-/-}$ MEFs had a faster prophase-telophase transition (Figures 4D and 4E) and demonstrated that the major difference between *Lzts1*$^{+/+}$ and *Lzts1*$^{-/-}$ cells was indeed the time needed to complete prophase (Figure 4E).

We next tested the effects of two different compounds able to block cells in prometaphase on *Lzts1* WT and KO MEFs. Both nocodazole- or taxol-treated *Lzts1*$^{-/-}$ cells failed to properly arrest in prometaphase (Figure 4F), and taxol- or nocodazole-treated *Lzts1*$^{-/-}$ MEFs displayed a lower percentage of abnormal mitotic figures (Blajeski et al., 2002) compared to *Lzts1*$^{+/+}$ cells (Figures 4G and 4H), consistent with an altered drug-induced M phase block.

Lzts1 Contributes to the Regulation of Cdk1 Activity during Mitosis

Once it had been defined that Lzts1 absence principally affects the transition from prophase to anaphase, we tested whether it influenced Cdk1 activity during M phase. To this purpose, Cdk1 was immunoprecipitated from *Lzts1*$^{+/+}$ and *Lzts1*$^{-/-}$ MEFs isolated by mitotic shake-off or treated with nocodazole and taxol, and its kinase activity was tested in an in vitro assay. Interestingly, levels of phosphorylated histone-H1 by Cdk1 were lower in mitotic *Lzts1*$^{-/-}$ MEFs (Figure 5A) and in nocodazole- or taxol-treated *Lzts1*$^{-/-}$ cells (Figure 5B). Similarly, in MEFs released from serum starvation, Cyclin B1 activity (Figure S2A; see the Supplemental Data available with this article online) and, in nocodazole-synchronized cells, Cdk1 activity (Figure S2B) dropped sooner in *Lzts1*$^{-/-}$ cells than in their WT counterparts. Altogether, these data indicate that, during mitosis, *Lzts1* absence resulted

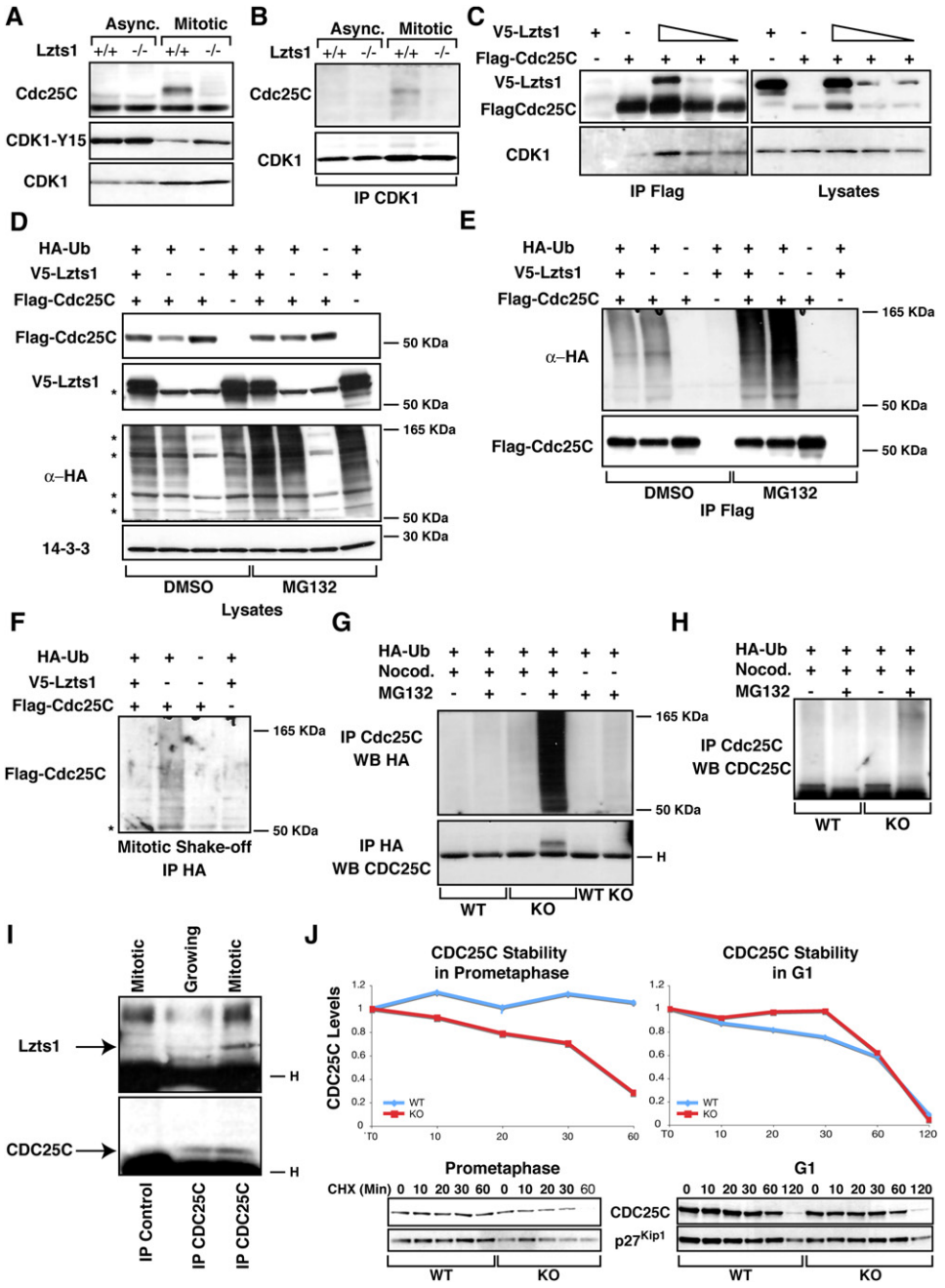

Figure 6. Loss of Lzts1 Impairs the Cdk1/Cdc25C Interaction in Mitotic Cells

(A) Western blot analysis of Cdc25C, Cdk1, and Cdk1-pY15 proteins in asynchronously growing (Async.) or in mitotic (Mitotic) *Lzts1*$^{+/+}$ and *Lzts1*$^{-/-}$ MEFs.

(B) Western blot analysis of Cdc25C and Cdk1 in lysates from *Lzts1*$^{+/+}$ and *Lzts1*$^{-/-}$ MEFs as in (A), immunoprecipitated with anti-Cdk1 antibody.

(C) Western blot analysis of hLzts1, hCdc25C, and hCdk1 in lysates (right panels) and Flag-IP (left panels) in 293 cells transfected with Flag-hCdc25C and increasing amounts of V5-hLzts1.

(D) Expression of hLzts1 and hCdc25C proteins in 293 cells transfected with the indicated vectors and treated with nocodazole for 6 hr in the presence or absence of the proteasome inhibitor MG132 (25 μM). Expression of Ha-Ub and 14-3-3 proteins was used as loading control.

(E) Cell lysates described in (D) were immunoprecipitated with an anti-Flag antibody and were analyzed for Ha-Ub and Cdc25C expression.

(F) 293 cells treated as in (D) were isolated by mitotic shake-off, and cell lysates were immunoprecipitated with an anti-Flag-HA antibody and were analyzed for Cdc25C expression.

(G) Proteins from *Lzts1*$^{+/+}$ and *Lzts1*$^{-/-}$ fibroblasts transduced with HA-Ub and hCdc25C retroviruses and then isolated by mitotic shake-off were immunoprecipitated with either an anti-Cdc25C or an anti-HA antibody and probed for HA-Ub or Cdc25C expression as indicated.

(H) Proteins from *Lzts1*$^{+/+}$ and *Lzts1*$^{-/-}$ fibroblasts treated as in (G) were immunoprecipitated and probed with an antibody specific for the Cdc25C phosphatase. An asterisk indicates nonspecific bands.

in a lower Cdk1 activity coupled with a faster prophase progression.

The time to complete mitosis represents an important variable in the execution of proper DNA separation (Cimini et al., 2003), and it has been demonstrated that decreasing Cdk1 activity in mitosis-arrested cells results in prompt mitotic exit accompanied by defects in DNA segregation (Seong et al., 2003; Niiya et al., 2005; Potapova et al., 2006).

We looked at the functional consequences of the faster mitotic exit accompanied by the lower Cdk1 activity observed in *Lzts1*$^{-/-}$ cells. Immunofluorescence analysis showed a 5-fold increase (4.5% in *Lzts1*$^{+/+}$ versus 26.1% in *Lzts1*$^{-/-}$ MEFs) in the number of cells containing lagging chromosomes during undisturbed mitosis in the absence of *Lzts1* (Figures 5C and 5D; Figure S1). This observation was further confirmed by the 4.5-fold increase in the percentage of cells with micronuclei in *Lzts1*$^{-/-}$ MEFs released after the thymidine block (Figures S1C and S1D). Moreover, after 3 or 4 days of nocodazole treatment, *Lzts1*$^{-/-}$ cells showed an increased hypertetraploid population (Figure 5E).

Overall, these data demonstrated that Lzts1 absence shortened M phase length and determined a decrease of Cdk1 activity during mitosis accompanied by increased chromosomes missegregation.

Lzts1 Is Necessary for Proper Cdk1/Cdc25C Interaction during Mitosis

How Lzts1 absence decreases Cdk1 activity as well as whether reduced kinase activity was responsible for the mitotic defects were investigated. Cdk1 activity is regulated by cyclin binding and phosphorylation of specific residues. Among the latter, a key role has been proposed for T14/Y15 phosphorylation by Wee1/Myt kinases and for dephosphorylation by Cdc25 phosphatases (Smits and Medema, 2001). Neither Cdk1 nor Cyclin B1 levels were significantly different (Figures 2D, 3B, and 5B) in WT and KO cells. Conversely, a higher Cdk1-pY15/Cdk1 ratio (Figure 6A) accompanied by lower levels of endogenous Cdc25C phosphatase was observed in mitotic *Lzts1*$^{-/-}$ MEFs (Figure 6A). Importantly, the different Cdc25C expression resulted in lower levels of endogenous Cdc25C associated with endogenous Cdk1 in mitotic *Lzts1*$^{-/-}$ MEFs (Figure 6B), evidence that could explain the higher Cdk1-pY15 phosphorylation and the lower Cdk1 activity.

A functional link between Lzts1 and Cdc25C expression was sought by transfecting 293 cells that were nocodazole synchronized in prometaphase with Flag-hCdc25C alone or with increasing amounts of V5-hLzts1. hCdc25C and hLzts1 coprecipitated (Figure 6C), and the increased expression of hLzts1 resulted in increased interaction between hCdc25C and endogenous Cdk1 (Figure 6C, lower panel). It has been proposed that in G2/M-arrested cells, hCdc25C may be efficiently ubiquitinated (Chen et al., 2002). To verify whether Lzts1 expression might control Cdc25C ubiquitination, cells were transfected with Flag-hCdc25C with or without V5-hLzts1 and were then nocodazole synchronized in the presence or absence of the proteasome inhibitor MG132. MG132 did not increase hCdc25C levels when hLzts1 was overexpressed, but it did increase levels in its absence (data not shown and Figure 6D). The same experiment was repeated with inclusion of a plasmid encoding an HA-tagged ubiquitin (HA-Ub) (Figures 6D and 6E). Data show that overexpression of Lzts1 reduced Cdc25C ubiquitination in 293 cells treated with nocodazole (Figure 6E). Moreover, 293 cells, transfected as described above, were isolated by mitotic shake-off, and cell lysates were immunoprecipitated with an anti-HA antibody to collect the ubiquitinated proteins. In mitotic cells, Lzts1 expression strongly decreased the ubiquitinated levels of Cdc25C (Figure 6F). In order to verify these observations in a more physiological system, hCdc25C and HA-Ub were retrovirally transduced into *Lzts1*$^{+/+}$ and *Lzts1*$^{-/-}$ fibroblasts treated or not treated with nocodazole in the presence or absence of MG132. Increased Cdc25C ubiquitination was observed in *Lzts1*$^{-/-}$ cells compared to parental cells (Figures 6G and 6H).

To confirm the physiological significance of the described interaction, we precipitated the endogenous Cdc25C protein from mitotic or exponentially growing 293 cells known to express high levels of Lzts1 (Ishii et al., 2001). In these conditions, endogenous Lzts1 readily associated with Cdc25C protein, preferentially in mitotic cells (Figure 6I). Moreover, analysis of the stability of the endogenous Cdc25C protein, evaluated by cycloheximide treatment, showed a decrease in *Lzts1*$^{-/-}$ only when cells were arrested in prometaphase, not when cycloheximide was added after the cells had returned to G1 phase (Figure 6J). In addition, we examined proteins from the mitotic fraction of a panel of human carcinoma cell lines that showed low Lzts1 expression to be associated with low levels of Cdc25C protein (Figure S3A) and with an increased phosphorylation of Cdk1 on Y15 when compared with normal mammary epithelial cells or 293 cells (Figures S3B and S3C). Importantly, reintroduction of Lzts1 in several Lzts1-deficient cells by using different technical approaches resulted in increased levels of Cdc25C only when the cells were isolated by mitotic shake-off (Figure S4).

Accordingly, hLzts1 re-expression in *Lzts1*$^{-/-}$ cells increased levels of Cdc25C protein (Figure 7A) and decreased levels of phosphorylated Cdk1-pY15 in mitotic cells (Figure 7A). Importantly, Lzts1 re-expression in *Lzts1*$^{-/-}$ MEFs rescued the sensitivity to taxol and nocodazole (Figures 7D and 7E), indicating that the observed

(I) Proteins from 293T cells isolated from exponentially growing or mitotic cells were immunoprecipitated with an antibody specific for the Cdc25C phosphatase (or control antibody) and were probed for Lzts1 (upper panel) and Cdc25C (lower panel).
(J) Cdc25C stability in mitotic (left panels) or G1 (right panels) cells. The protein stability of Cdc25C was analyzed in prometaphase cells (nocodazole arrested) and in asynchronous cells by treatment with cycloheximide for the indicated time points (min). Quantification of protein expression was obtained by scanning the blots with the Biorad GS100 scanner interfaced with the Quantity One software.

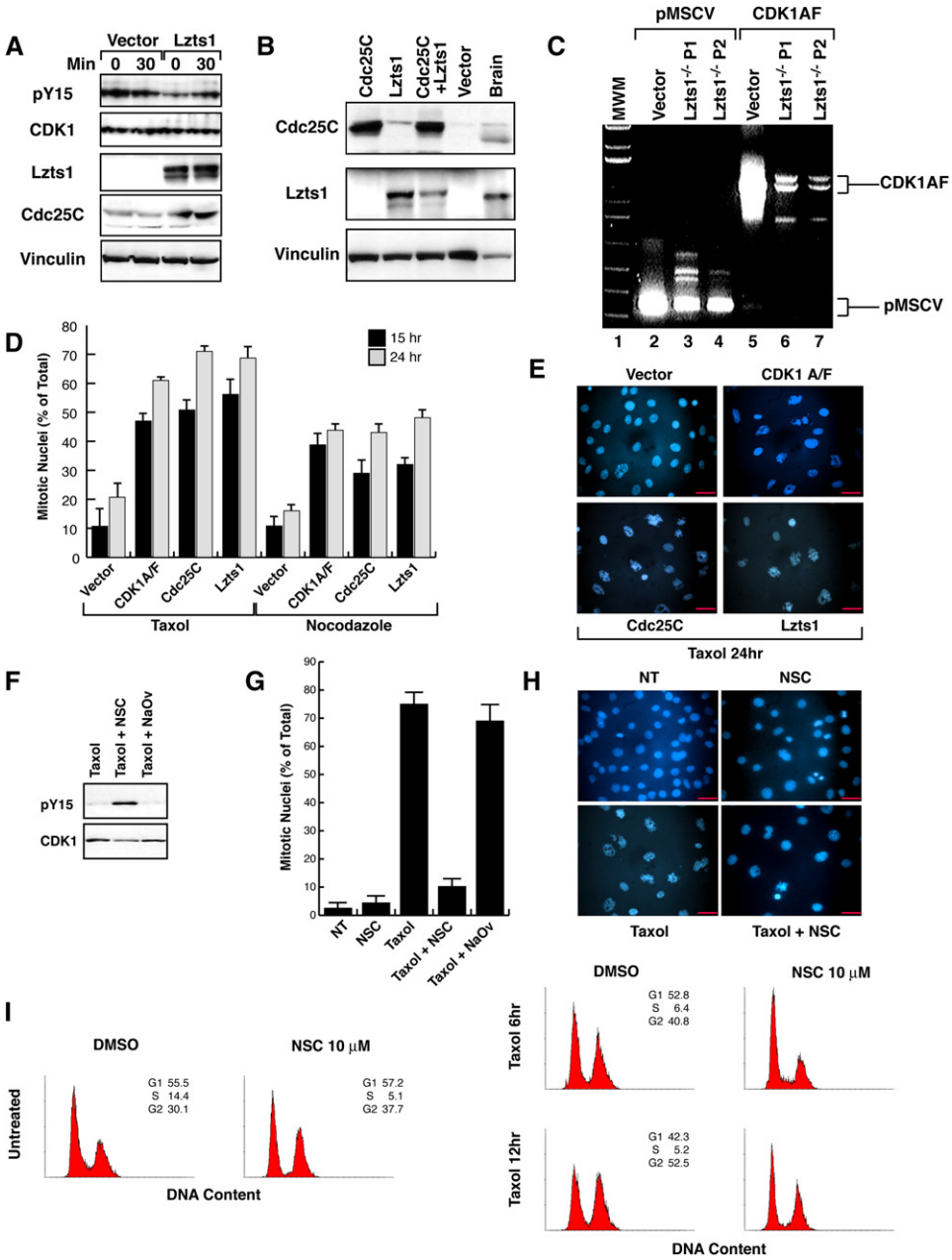

Figure 7. Regulation of Cdc25C Activity by Lzts1 Is Necessary for Proper Mitotic Progression

(A) Western blot analysis of Cdk1-pY15, Cdk1, Cdc25C, Lzts1, and vinculin (loading control) proteins in mitotic *Lzts1*$^{-/-}$ MEFs transduced with an empty vector or with a vector encoding for the Lzts1 protein. Lysates were collected 0 or 30 min after the mitotic shake-off.

(B) Western blot analysis of Cdc25C, Lzts1, and vinculin (loading control) proteins in *Lzts1*$^{-/-}$ MEFs transduced with the indicated vectors. Mouse brain lysate was used as a positive control for Lzts1 expression.

(C) RT-PCR analysis of Cdk1AF expression in *Lzts1*$^{-/-}$ MEFs transduced as indicated. The transduced DNA plasmids (vector) were used as positive controls.

(D and E) Evaluation of mitotic nuclei in *Lzts1*$^{-/-}$ MEFs transduced as indicated. Typical fields of Hoechst nuclear staining are shown in (E), and the mean of three independent experiments is reported in (D).

(F) Western blot analysis of Cdk1 and Cdk1-pY15 expression in *Lzts1*$^{+/+}$ MEFs treated for 1 hr with DMSO (NT), NSC, or Na_3VO_4 and then with taxol for 18 hr.

(G and H) Evaluation of mitotic nuclei in *Lzts1*$^{+/+}$ MEFs treated as in (F). Data (mean ± SD) represent the mean of a least three independent experiments performed in duplicate.

(I) Flow cytometry analysis of *Lzts1*$^{+/+}$ and *Lzts1*$^{-/-}$ MEFs treated with vehicle (DMSO) or 10 μM NSC for 1 hr and then, after the NSC washout, exposed to 100 nM taxol for the indicated time. Scale bars are 20 μm.

differences between *Lzts1* WT and KO cells could be ascribed to the absence of Lzts1 protein.

To further test the role of Cdc25C in the mitotic phenotype observed in Lzts1 null fibroblasts, we retrovirally transduced *Lzts1*$^{-/-}$ cells with Cdc25C (Figure 7B) or with a nonphosphorylable form of Cdk1 protein (Cdk1AF) (Figure 7C). In the absence of Lzts1, both Cdc25C and Cdk1AF expression resulted in a reacquisition of sensitivity to a taxol- and nocodazole-induced M phase block (Figures 7D and 7E). Overall, these data suggest that the Lzts1/Cdk1/Cdc25C pathway represents a key control for the proper execution of M phase.

To verify whether Cdc25C deregulation in WT cells could recapitulate the phenotype observed in *Lzts1* null cells, we used the Cdc25C inhibitor NSC 663284 (NSC) (Chao et al., 2004; Han et al., 2004). Like *Lzts1* null MEFs, *Lzts1*$^{+/+}$ MEFs treated with NSC for 1 hr and then washed and exposed to taxol showed increased Cdk1-pY15 phosphorylation levels (Figure 7F) and overcame the taxol-dependent M phase block (Figures 7G–7I). The nonspecific phosphatase inhibitor sodium orthovanadate ($NaVO_4$) had no effect on either Cdk1-pY15 phosphorylation or taxol-induced mitotic block (Figures 7F and 7G).

Lzts1-Deficient MEFs Are Prone to Transformation

How can the observed mitotic defects be linked to the increased tumor incidence noted in *Lzts1* KO mice? We speculated that since *Lzts1*$^{-/-}$ MEFs showed altered chromosome segregation (Figure 5C; Figure S1), they could be more prone to transformation due to the accumulation of genetic abnormalities. To test this hypothesis, WT and KO *Lzts1* MEFs were retrovirally infected with a Ha-Ras (V12) vector (Figure S5A), selected in hygromycin, and assayed for the ability to form colonies in soft agar. Only *Lzts1*$^{-/-}$ MEFs formed colonies (Figure S5B), an effect independent of the silencing of the p19^{Arf} tumor-suppressor gene (Figure S5), confirming that Lzts1 absence conferred a tumor-prone phenotype to mouse cells.

High Incidence of NMBA-Induced Forestomach Tumors in *Lzts1*-Deficient Mice

We also tested whether this observation could be recapitulated in in vivo experiments. Since the *LZTS1* gene is often downregulated in esophageal carcinomas (Ishii et al., 1999), and since epidemiological studies have linked exposure to *N*-nitrosomethylbenzylamine (NMBA) with an increased incidence of esophageal cancer (Yang, 1980; Magee, 1989), NMBA treatment was used to determine whether *Lzts1* modulates carcinogen-induced malignancy development. A total of 6 weeks after NMBA administration, all 20 *Lzts1*$^{-/-}$ mice (100%) and all 33 *Lzts1*$^{+/-}$ mice (100%) developed multiple tumors of the forestomach (Figure 8), whereas only 5 of 30 *Lzts1*$^{+/+}$ mice (17%) developed tumors (*Lzts1*$^{+/+}$ versus *Lzts1*$^{-/-}$, $p < 0.001$; *Lzts1*$^{+/+}$ versus *Lzts1*$^{+/-}$, $p < 0.001$).

Histological sections showed an array of lesions typically seen in NMBA-treated animals, including hyperplasia, focal hyperplastic lesions, papillomas, and carcinomas. *Lzts1*$^{-/-}$ and *Lzts1*$^{+/-}$ mice developed invasive carcinoma of the forestomach at a high frequency, while *Lzts1*$^{+/+}$ mice mostly showed thin and regular epithelia (Figure 8). All *Lzts1*$^{+/-}$ mice retained the WT allele (Figure 8) that was negative for mutations (data not shown), suggesting haploinsufficiency of *Lzts1*, as supported by the fact that *Lzts1* heterozygous mice developed spontaneous tumors retaining the normal allele.

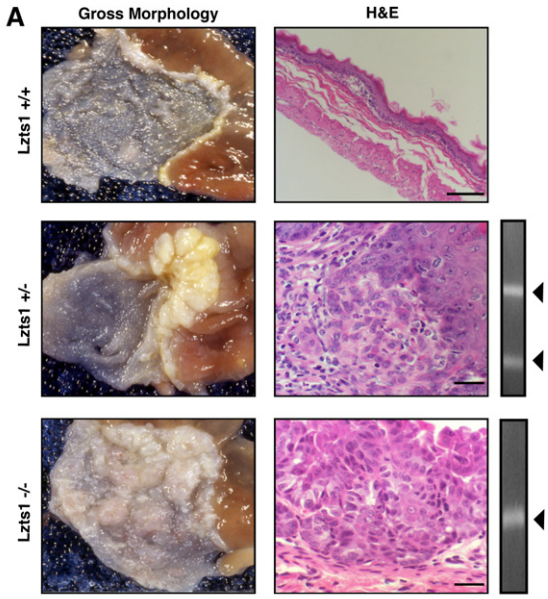

B

Average Tumor number and incidence of Lzts1 mice after NMBA treatment

Mice Genotype	Animal Number	Carcinogen Administration	Tumor Incidence (%)	Tumor number per mouse
Lzts1 (+/+)	30	(+)	5/30(17%)	0.4 (9/30)
	7	(-)	0/7 (0%)	0 (0/7)
Lzts1 (+/-)	33	(+)	33/33 (100%)	2.7 (90/33)
	8	(-)	0/8 (0%)	0 (0/5)
Lzts1 (-/-)	20	(+)	20/20(100%)	5.8 (116/20)

Figure 8. Loss of *Lzts1* Enhances NMBA-Induced Forestomach Carcinogenesis in Mice

(A) Left panels: gross morphology of the forestomach and SCJ in *Lzts1*$^{+/+}$, *Lzts1*$^{+/-}$, and *Lzts1*$^{-/-}$ mice (top to bottom, 35×). Middle panels: hematoxylin and eosin stained forestomach sections. Normal epithelium is shown in *Lzts1*$^{+/+}$; early infiltrating carcinomas and infiltrating carcinomas are shown in *Lzts1*$^{+/-}$ and *Lzts1*$^{-/-}$ mice. The scale bars are 100 μm in upper panel and 20 μm in lower panels. Right panels: retention of the remaining WT allele in a tumor from heterozygous mice. (B) Number and incidence of induced tumors in the different genotypes.

DISCUSSION

The present study demonstrates how inactivation of one or both *Lzts1* alleles causes an increased incidence of either spontaneous or carcinogen-induced tumors in mice.

The development of spontaneous tumors from different organs suggests that Lzts1 absence interferes with important pathways in normal cell homeostasis.

Besides the appearance of spontaneous tumors of different origins, we demonstrated that the absence of endogenous *Lzts1* results in increased tumor susceptibility of the forestomach after NMBA treatment (present work) and of the bladder after N-butyl-N-(4-hydroxybutyl) nitrosamine (BBN) administration (A.V. and C.M.C., unpublished data), further suggesting that Lzts1 absence sensitizes multiple tissues to carcinogenesis. In both cases, loss of one *Lzts1* allele effectively predisposes mice to carcinogenesis, since, in fact, no loss of the WT *Lzts1* allele or mutation in the *Lzts1* coding region was found. Therefore, the *Lzts1* gene could be haploinsufficient in tumor suppression, as already demonstrated for other tumor-suppressor genes, like *p53* (Venkatachalam et al., 1998), $p27^{kip1}$ (Fero et al., 1998), or *Pten* (Kwabi-Addo et al., 2001).

The tumor-prone phenotype of *Lzts1* KO mice is consistent with the role of Lzts1 protein in the control of M phase progression described here. Aneuploidy has been strictly linked to human cancer, and it is increasingly accepted that weakened M phase checkpoints likely result in aneuploidy and tumor progression (Weaver and Cleveland, 2005). The finding in *Lzts1* null cells of a higher number of missegreagated chromosomes is consistent with the Lzts1 tumor-suppressor role in several tissues in vivo. The relative late onset of spontaneous tumors observed in *Lzts1* KO mice could be explained by the high apoptotic rate of *Lzts1*-deficient MEFs. Accordingly, in spleens of 5- to 6-month-old mice (n = 4 WT and 5 KO), there is a 5-fold increase in the amount of the caspase-3-negative nuclear fragment (20.25 ± 4.2 versus 4.4 ± 2 × high-power field [HPF]; n = 100 HPF), which represents engulfed apoptotic bodies or cells that died as a result of mitotic catastrophe after unsuccessful cell division (Figure S6).

The present work demonstrates that Lzts1 protein expression is critical for normal mitosis progression. Lzts1 absence shortens the mitotic division time and causes improper chromosome segregation, lowering Cdk1 activity through Cdc25C destabilization. The classical view of M phase entrance and progression implicates a central role for Cdk1 and Cdc25C, with high Cdk1 activity necessary for the proper execution of M phase (reviewed in Jackson, 2006). However, several experimental evidences suggest that the loss of Cdk1 activity primarily drives the exit from mitosis, data arguing that Cdk1 inactivation serves as a mechanism for ensuring the correct timing of mitosis exit (Potapova et al., 2006; Cross et al., 2005; Parry and O'Farrell, 2001; Sigrist et al., 1995; Chang et al., 2003). The activity of Cdk1 upon mitosis entry is higher than what is needed to maintain the M phase. Such a hysteric loop likely depends on Cdk1 phosphorylation levels, rather than on cyclin expression (Sha et al., 2003). Accordingly, the depletion of Greatwall kinase from *Xenopus* mitotic extract induced a prompt exit from M phase with an increase of Cdk1-pY15 phosphorylation, likely the result of Cdc25C inactivation rather than Cyclin B1 degradation (Yu et al., 2006). This observation is consistent with the fact that pharmacological inhibition of Cdk1 in mitotic cells determines a prompt exit from mitosis, even in the presence of proteasome inhibitors or prometaphase actin drugs (Seong et al., 2003; Niiya et al., 2005; Potapova et al., 2006; Vassilev et al., 2006). Since Cyclin B1 degradation is necessary for the onset of anaphase (Chang et al., 2003) and starts as soon as the chromosomes align at the metaphase plate (Clute and Pines, 1999), decreased Cdk1 activity via changes in its inhibitory phosphorylation could lead to mitotic exit in the window between prophase and metaphase, during which Lzts1 seems to principally act.

It has recently been reported that Cdc25 phosphatases play different roles in the execution of proper M phase progression: Cdc25A and Cdc25B are necessary for M phase entry, and Cdc25C plays a more prominent role in the proper execution of prophase (Lindqvist et al., 2005). This finding is in agreement with our observation that the Lzts1/Cdc25C interaction mainly impairs prophase length rather than M phase entrance. Whether the Lzts1/Cdc25C interaction is dependent on the presence of other proteins or on Lzts1 and/or Cdc25C phosphorylation is an issue that will be investigated in future studies. However, the data presented here add another piece in the complex regulation of mitosis progression and suggest that the control of protein degradation during M phase governs the progression from prophase to metaphase, thus going beyond the regulation of the anaphase-cytokinesis transition driven by the activation of the Anaphase Promoting Complex.

Collectively, our data and the current literature suggest that decreasing Cdk1 activity in interphase cells may result in the G2 block of the cell cycle, whereas decreasing Cdk1 activity in M phase before the establishment of the metaphase plate may cause a faster prometaphase progression and mitotic exit, as seen in $Lzts1^{-/-}$ cells. Interestingly, this hypothesis has recently been experimentally proven in human cell lines by using a new selective Cdk1 inhibitor (Vassilev et al., 2006).

In the present work, we show that Lzts1 contributes to the maintenance of high levels of Cdk1 activity during M phase, preventing chromosomes missegregation. This important function of Cdk1 has been recently demonstrated by the use of Cdk1-specific inhibitors. The sudden drop of Cdk1 activity in prometaphase-arrested cells results in chromosomes missegregation and the formation of aneuploid progeny (Seong et al., 2003; Vassilev et al., 2006).

In complete agreement with this view, KO of the RASSF1A protein shortened prometaphase length by prematurely inducing Cyclin B1 degradation and led to the appearance of misaligned chromosomes. As a consequence, RASSF1A null cells are more prone to cell transformation (Song et al., 2004). Thus, two independent studies support the hypothesis that there may exist proteins (i.e., Lzts1 and RASSF1A) able, by different mechanisms, to ensure that Cdk1 activity remains high until the metaphase plate is formed. The absence of such regulators

results in a similar tumor-prone phenotype linked to chromosome missegregation, suggesting that a fine regulation of Cdk1 activity is necessary not only for M phase entrance and exit, but also for the progression from prometaphase to metaphase. Accordingly, our preliminary data suggest that Lzts1 overexpression in mammary carcinoma cells leads to an increased number of M phase-arrested cells that eventually die by apoptosis or mitotic catastrophe for an unsuccessful cell division (G.B. and C.M.C., unpublished data). Similarly, RASSF1A overexpression results in M phase block at prometaphase, followed by cell death (Song et al., 2004). The involvement in this type of regulation of two proteins that regulate protein degradation and bind the microtubules, Lzts1 (Ishii et al., 2001) and RASSF1A (Song et al., 2004), suggests that the spatial organization of the cyclin/Cdk1 complex is also important to achieveme proper activation of the complex, an issue that needs further work to be clarified.

In conclusion, our work points to *Lzts1* as an important player in the execution of normal M phase progression. Moreover, we show that the absence of *Lzts1* leads to impaired chromosome segregation, cell transformation, and cancer progression, and that mice lacking *Lzts1* are an important tool by which to study mitosis progression, cancer etiology, and resistance to anticancer therapy.

EXPERIMENTAL PROCEDURES

Mouse *Lzts1* Gene Targeting and Mating

Generation of knockout mice for Lzts1 is better described in Supplemental Experimental Procedures.

Expression Vectors

The human *CDC25C* cDNA, inserted in the pOTB7 vector, was purchased from "MAMMALIAN GENE COLLECTION" American Type Culture Collection. The *CDC25C* cDNA was subcloned in the pFlag-CMV 6a expression vector (Sigma). For retroviral expression, *LZTS1*, *CDC25C*, and *CDK1AF* cDNAs were cloned in pMSCV-Puro vector (Clontech) without any tag. The pHA-Ubiquitin, the pMSCV-Ha-Ras, and the pHA-*CDK1AF* expression vectors are kind gifts of Prof. A. Morrione, R. Baserga, and G. Draetta, respectively.

Cell Cultures and Treatments

MEFs were derived from 13.5-day-old embryos as previously described (McCurrach and Lowe, 2001). Briefly, after removal of the head and internal organs, embryos were rinsed with phosphate-buffered saline (PBS), minced, and resuspended in DMEM containing 10% FBS and 2 mM glutamine, 0.1 mM MEM nonessential amino acids, and 100 IU/ml penicillin and 100 μg/ml streptomycin. Cell media and reagents were obtained from GIBCO-BRL, except where noted. Cells from single embryos were plated into one 100 mm culture dish (Falcon) and incubated at 37°C in a 5% CO_2-humidified chamber. Plating after disaggregation of embryos was considered passage 0, and the first replating 3 days later was considered passage 1. All of the experiments were performed by using cells between passages 2 and 10 from three different batches. Genotypes of MEFs were verified by RT-PCR and Southern blot analysis.

For retroviral transduction of proliferating primary MEFs, high-titer viruses were produced from EcoPack293 (Clontech) transfected with pMSCV vectors by the calcium-phosphate precipitation technique. Stable, mass-transduced MEF populations were selected in Hygromycin B (400 μg/ml) or Puromycin (1.5 μg/ml), and the effective expression of the transduced proteins was always confirmed by western blot analysis and by RT-PCR with the appropriate MSCV primers (Clontech).

MEF synchronization in the different phases of the cell cycle as well as treatments are better described in Supplemental Experimental Procedures.

Immunoprecipitation, Immunoblotting, and Immunocytochemistry

Procedures for protein analysis by immunoprecipitation, immunoblotting, and immunocytochemistry are described in Supplemental Experimental Procedures and were essentially performed as previously described (Baldassarre et al., 2005).

Time-Lapse Experiments

Monitoring of cell mitosis was carried out on double-thymidine-blocked and nonblocked cells. For the double-thymidine block, 30%–40% confluent cells, seeded in 35 mm diameter Petri dishes, were incubated with 2 mM thymidine for 14–16 hr at 37°C. After incubation, cells were rinsed with PBS and incubated with thymidine-free medium for 10 hr. Then, cells were split 1:2 and reincubated with 2 nM thymidine for 18 hr. After 5 hr of block, cell mitosis was followed with time-lapse cinematography, by using Image Analysis Software (Discovery-1, Universal Imaging, USA). Nonblocked cells were starved overnight with DMEM-0.1% FBS before time-lapse analysis.

The apparatus for time-lapse experiments consisted of an inverted microscope (IX50 Olympus), a CCD coolsnap camera (RS Photometrix, USA), an x-y-z computer-controlled stage, PROSCAN (Prior, USA), and a mini-incubator set on the stage. The camera and the computerized stage were synchronized by a specific code to follow several cells in the same experiment. Cells were observed for 7–12 hr, and images were acquired every 1 or 2 min. Movies were realized from the acquired images and were analyzed by Metamorph off-line software.

Animal Experiments

Eleven- to twelve-week-old $Lzts1^{+/-}$, $Lzts1^{-/-}$, or $Lzts1^{+/+}$ mice, which were produced in the Thomas Jefferson University animal facility, were given two intragastric doses of NMBA (Ash Stevens, Inc.) over the course of 1 week at 2 mg/kg body weight. All mice were sacrificed 6 weeks after NMBA doses. Animal experiments were conducted after approval of the Institutional Animal Care and Use Committee, Thomas Jefferson University.

Tumor Microdissection and DNA and RNA Analysis

Tumor microdissection and DNA amplification were performed as described previously (Bai et al., 2003), after minor modification. Briefly, 15 μm sections adhered on slides were deparaffinized, and the lesions were scraped off the sections so that they could be separated from normal tissue. The material obtained was then digested in DNA digestion buffer with the addition of 200 μM proteinase K. The murine *Lzts1* contains three coding exons that were amplified and sequenced with three pairs of primers (available upon request). PCR products were subjected to direct sequencing after purification through a QIAquick column (QIAGEN). RT-PCR was performed with a Superscript cDNA synthesis system (GIBCO-BRL). PCR amplification was performed with primers (available upon request) corresponding to the 5′ and 3′ margins of exon 1.

The cDNA was amplified by using glucose-3-phosphate dehydrogenase primers (Clontech) as controls.

Statistical Evaluation

A biostatistic program (GraphPad Software, Inc., San Diego, CA) was used for statistical analysis. Tumor incidence differences were analyzed by a two-sided Fisher's exact test. All statistical tests were two sided and were considered to be statistically significant at $p < 0.05$.

Supplemental Data

The Supplemental Data include Supplemental Experimental Procedures and six supplemental figures and are available at http://www.cancercell.org/cgi/content/full/11/3/275/DC1/.

ACKNOWLEDGMENTS

This work was supported partially by the Associazione Italiana per la Ricerca sul Cancro (A.V. and G.B.); the Programma Oncotecnologico, Istituto Superiore di Sanita (A.V.); the Ministero della Salute (A.V. and G.B.); and by National Cancer Institute grants (C.M.C). We thank Paolo Carboni at the University Federico II, Naples, and Sara D'Andrea at the Centro di Riferimento Oncologico, Aviano for excellent technical assistance.

Received: July 17, 2006
Revised: November 29, 2006
Accepted: January 11, 2007
Published: March 12, 2007

REFERENCES

Anbazhagan, R., Fujii, H., and Gabrielson, E. (1998). Allelic loss of chromosomal arm 8p in breast cancer progression. Am. J. Pathol. *152*, 815–819.

Bai, F., Pei, X.H., Godfrey, V.L., and Xiong, Y. (2003). Haploinsufficiency of $p18^{INK4c}$ sensitizes mice to carcinogen-induced tumorigenesis. Mol. Cell. Biol. *23*, 1269–1277.

Baldassarre, G., Belletti, B., Nicoloso, M.S., Schiappacassi, M., Vecchione, A., Spessotto, P., Morrione, A., Canzonieri, V., and Colombatti, A. (2005). p27(Kip1)-stathmin interaction influences sarcoma cell migration and invasion. Cancer Cell *7*, 51–63.

Blajeski, A.L., Phan, V.A., Kottke, T.J., and Kaufmann, S.H. (2002). G1 and G2 cell-cycle arrest following microtubule depolymerization in human breast cancer cells. J. Clin. Invest. *110*, 91–99.

Cabeza-Arvelaiz, Y., Sepulveda, J.L., Lebovitz, R.M., Thompson, T.C., and Chinault, A.C. (2001). Functional identification of LZTS1 as a candidate prostate tumor suppressor gene on human chromosome 8p22. Oncogene *20*, 4169–4179.

Carnero, A. (2002). Targeting the cell cycle for cancer therapy. Br. J. Cancer *87*, 129–133.

Chao, J.I., Kuo, P.C., and Hsu, T.S. (2004). Down-regulation of survivin in nitric oxide-induced cell growth inhibition and apoptosis of the human lung carcinoma cells. J. Biol. Chem. *279*, 20267–20276.

Chang, D.C., Xu, N., and Luo, K.Q. (2003). Degradation of cyclin B is required for the onset of anaphase in mammalian cells. J. Biol. Chem. *278*, 37865–37873.

Chen, F., Zhang, Z., Bower, J., Lu, Y., Leonard, S.S., Ding, M., Castranova, V., Piwnica-Worms, H., and Shi, X. (2002). Arsenite-induced Cdc25C degradation is through the KEN-box and ubiquitin-proteasome pathway. Proc. Natl. Acad. Sci. USA *99*, 1990–1995.

Cimini, D., Moree, B., Canman, J.C., and Salmon, E.D. (2003). Merotelic kinetochore orientation occurs frequently during early mitosis in mammalian tissue cells and error correction is achieved by two different mechanisms. J. Cell Sci. *116*, 4213–4225.

Clute, P., and Pines, J. (1999). Temporal and spatial control of cyclin B1 destruction in metaphase. Nat. Cell Biol. *1*, 82–87.

Cross, F.R., Schroeder, L., Kruse, M., and Chen, K.C. (2005). Quantitative characterization of a mitotic cyclin threshold regulating exit from mitosis. Mol. Biol. Cell *16*, 2129–2138.

El-Naggar, A.K., Coombes, M.M., Batsakis, J.G., Hong, W.K., Goepfert, H., and Kagan, J. (1998). Localization of chromosome 8p regions involved in early tumorigenesis of oral and laryngeal squamous carcinoma. Oncogene *16*, 2983–2987.

Fero, M., Randel, E., Gurley, K.E., Roberts, J.M., and Kemp, C.J. (1998). The murine gene $p27^{Kip1}$ is haplo-insufficient for tumor suppression. Nature *396*, 177–180.

Han, Y., Shen, H., Carr, B.I., Wipf, P., Lazo, J.S., and Pan, S. (2004). NAD(P)H:quinone oxidoreductase-1-dependent and -independent cytotoxicity of potent quinone Cdc25 phosphatase inhibitors. J. Pharmacol. Exp. Ther. *309*, 64–70.

Ichikawa, T., Nihei, N., Suzuki, H., Oshimura, M., Emi, M., Nakamura, Y., Hayata, I., Isaacs, J.T., and Shimazaki, J. (1994). Suppression of metastasis of rat prostatic cancer by introducing human chromosome 8. Cancer Res. *54*, 2299–2302.

Ishii, H., Baffa, R., Numata, S., Murakumo, Y., Rattan, S., Inoue, H., Mori, M., Fidanza, V., Alder, H., and Croce, C.M. (1999). The *FEZ1* gene at chromosome 8p22 encodes a leucine-zipper protein, and its expression is altered in multiple human tumors. Proc. Natl. Acad. Sci. USA *96*, 3928–3933.

Ishii, H., Vecchione, A., Murakumo, Y., Baldassarre, G., Numata, S., Trapasso, F., Alder, H., Baffa, R., and Croce, C.M. (2001). FEZ1/LZTS1 gene at 8p22 suppresses cancer cell growth and regulates mitosis. Proc. Natl. Acad. Sci. USA *98*, 10374–10379.

Jackson, P.K. (2006). Climbing the Greatwall to mitosis. Mol. Cell *22*, 156–157.

Kwabi-Addo, B., Giri, D., Schimdt, K., Podsypanina, K., Parson, R., Greenberg, N., and Ittmann, M. (2001). Haploinsufficiency of Pten tumor suppressor gene promotes prostate cancer progression. Proc. Natl. Acad. Sci. USA *98*, 11563–11568.

Lindqvist, A., Kallstrom, H., Lundgren, A., Barsoum, E., and Rosenthal, C.K. (2005). Cdc25B cooperates with Cdc25A to induce mitosis but has a unique role in activating cyclin B1-Cdk1 at the centrosome. J. Cell Biol. *171*, 35–45.

Magee, P.N. (1989). The experimental basis for the role of nitroso compounds in human cancer. Cancer Surv. *8*, 207–239.

McCurrach, M.E., and Lowe, S.W. (2001). Methods for studying pro- and antiapoptotic genes in nonimmortal cells. Methods Cell Biol. *66*, 197–227.

McGarry, T.J., and Kirschner, M.W. (1998). Geminin, an inhibitor of DNA replication, is degraded during mitosis. Cell *93*, 1043–1053.

Nigg, E.A. (2001). Mitotic kinases as regulators of cell division and its checkpoints. Nat. Rev. Mol. Cell Biol. *2*, 21–32.

Niiya, F., Xie, X., Lee, K.S., Inoue, H., and Miki, T. (2005). Inhibition of cyclin-dependent kinase 1 induces cytokinesis without chromosome segregation in an ECT2 and MgcRacGAP-dependent manner. J. Biol. Chem. *280*, 36502–36509.

Nonaka, D., Fabbri, A., Roz, L., Mariani, L., Vecchione, A., Moore, G.W., Tavecchio, L., Croce, C.M., and Sozzi, G. (2005). Reduced FEZ1/LZTS1 expression and outcome prediction in lung cancer. Cancer Res. *65*, 1207–1212.

Ono, K., Uzawa, K., Nakatsuru, M., Shiiba, M., Mochida, Y., Tada, A., Bukawa, H., Miyakawa, A., Yokoe, H., and Tanzawa, H. (2003). Down-regulation of FEZ1/LZTS1 gene with frequent loss of heterozigosity in oral squamous cell carcinomas. Int. J. Oncol. *23*, 297–302.

Parry, D.H., and O'Farrell, P.H. (2001). The schedule of destruction of three mitotic cyclins can dictate the timing of events during exit from mitosis. Curr. Biol. *11*, 671–683.

Potapova, T.A., Daum, J.R., Pittman, B.D., Hudson, J.R., Jones, T.N., Satinover, D.L., Stukenberg, P.T., and Gorbsky, G.J. (2006). The reversibility of mitotic exit in vertebrate cells. Nature *440*, 954–958.

Seong, Y.S., Min, C., Li, L., Yang, J.Y., Kim, S.-Y., Cao, X., Kim, K., Yuspa, S.H., Chung, H.H., and Lee, K.S. (2003). Characterization of a novel cyclin-dependent kinase 1 inhibitor, BMI-1026. Cancer Res. *63*, 7384–7391.

Sha, W., Moore, J., Chen, K., Lassaletta, A.D., Yi, C.-S., Tyson, J.J., and Sible, J.C. (2003). Hysteresis drives cell-cycle transitions in *Xenopus laevis* egg extracts. Proc. Natl. Acad. Sci. USA *100*, 975–980.

Shuji, K., Gerburg, W., Masafumi, N., and Kun Ping, L. (2001). Telomeric protein Pin2/TRF1 induces mitotic entry and apoptosis in cells with short telomers and is down-regulated in human breast tumors. Oncogene *20*, 1497–1508.

Sigrist, S., Jacobs, H., Stratmann, R., and Lehner, C.F. (1995). Exit from mitosis is regulated by *Drosophila* fizzy and the sequential destruction of cyclins A, B and B3. EMBO J. *14*, 4827–4838.

Smits, V.A.J., and Medema, R.H. (2001). Checking out the G2/M transition. Biochim. Biophys. Acta *1519*, 1–12.

Song, M.S., Song, S.J., Ayad, N.G., Chang, J.S., Lee, J.H., Hong, H.K., Lee, H., Choi, N., Kim, J., Kim, H., et al. (2004). The tumour suppressor RASSF1A regulates mitosis by inhibiting the APC-Cdc20 complex. Nat. Cell Biol. *6*, 129–137.

Tobey, R.A., Oishi, N., and Crissman, H.A. (1990). Cell cycle synchronization: reversible induction of G2 synchrony in cultured rodent and human diploid fibroblasts. Proc. Natl. Acad. Sci. USA *87*, 5104–5108.

Toyooka, S., Fukuyama, Y., Wistuba, I.I., Tockman, M.S., Minna, J.D., and Gazdar, A.F. (2002). Differential expression of FEZ1/LZTS1 gene in lung cancers and their cell cultures. Clin. Cancer Res. *8*, 2292–2297.

Vassilev, L.T., Tovar, C., Chen, S., Knezevic, D., Zhao, X., Sun, H., Heimbrook, D.C., and Chen, L. (2006). Selective small-molecule inhibitor reveals critical mitotic functions of human CDK1. Proc. Natl. Acad. Sci. USA *103*, 10660–10665.

Vecchione, A., Ishii, H., Shiao, Y.-H., Trapasso, F., Rugge, M., Alder, H., Croce, C.M., and Baffa, R. (2001). Altered expression of Fez1 protein in gastric carcinoma. Clin. Cancer Res. *7*, 1546–1552.

Vecchione, A., Ishii, H., Baldassarre, G., Bassi, P., Trapasso, F., Alder, H., Pagano, F., Gomella, L.G., Croce, C.M., and Baffa, R. (2002). FEZ1/LZTS1 is down-regulated in high-grade bladder cancer, and its restoration suppresses tumorigenicity in transitional cell carcinoma cells. Am. J. Pathol. *160*, 1345–1352.

Venkatachalam, S., Shi, Y.P., Jones, S.N., Vogel, H., Bradley, A., Pinkel, D., and Donehower, L.A. (1998). Retention of wild-type p53 in tumors from p53 heterozygous mice: reduction of p53 dosage can promote cancer formation. EMBO J. *17*, 4657–4667.

Vocke, C.D., Pozzatti, R.O., Bostwick, D.G., Florence, C.D., Jennings, S.B., Strup, S.E., Duray, P.H., Liotta, L.A., Emmert-Buck, M.R., and Linehan, W.M. (1996). Analysis of 99 microdissected prostate carcinomas reveals a high frequency of allelic loss on chromosome 8p12–21. Cancer Res. *56*, 2411–2416.

Wagner, U., Bubendorf, L., Gasser, T.C., Moch, H., Gorog, J.P., Richter, J., Mihatsch, M.J., Waldman, F.M., and Sauter, G. (1997). Chromosome 8p deletions are associated with invasive tumor growth in urinary bladder cancer. Am. J. Pathol. *151*, 753–759.

Weaver, B.A.A., and Cleveland, D.W. (2005). Decoding the links between mitosis, cancer and chemotherapy. The mitotic checkpoint, adaptation and cell death. Cancer Cell *8*, 7–12.

Westendorf, J.M., Rao, P.N., and Gerace, L. (1994). Cloning of cDNAs for M-phase phosphoproteins recognized by the MPM2 monoclonal antibody and determination of the phosphorylated epitope. Proc. Natl. Acad. Sci. USA *91*, 714–718.

Yang, C.S. (1980). Research on esophageal cancer in China: a review. Cancer Res. *40*, 2633–2644.

Yu, J., Zhao, Y., Li, Z., Galas, S., and Goldberg, M.L. (2006). Greatwall kinase participates in the CDC2 autoregulatory loop in *Xenopus* egg extracts. Mol. Cell *22*, 83–91.

Accession Numbers

Coordinates have been deposited in the NCBI database with accession code AF288601.